Allosteric conformational spread: Exact results using a simple transfer matrix method

S. G. J. Mochrie,[1,2] A. H. Mack,[2] and L. Regan[3,4]
[1]*Department of Physics, Yale University, New Haven, Connecticut 06511, USA*
[2]*Department of Applied Physics, Yale University, New Haven, Connecticut 06520, USA*
[3]*Department of Molecular Biophysics and Biochemistry, Yale University, New Haven, Connecticut 06520, USA*
[4]*Department of Chemistry, Yale University, New Haven, Connecticut 06520, USA*
(Received 19 May 2010; published 23 September 2010)

A transfer matrix method is described for the conformational spread (CS) model of allosteric cooperativity within a one-dimensional arrangement of four-state binding sites. Each such binding site can realize one of two possible conformational states. Each of these states can either bind ligand or not bind ligand. Thus, analytical expressions that are exact within the context of the CS model are derived for the grand partition function, for the mean fraction of binding sites occupied by ligand versus ligand concentration, and for the mean fraction of binding sites in a given allosteric state versus ligand concentration. The utility of our analytical results is demonstrated by least-mean-square fitting of prior experimental results obtained on the bacterial flagellar motor for the fraction of FliM/FliG/FliN complexes with CheY-P bound [V. Sourjik and H. C. Berg, Proc. Natl. Acad. Sci. U.S.A. **99**, 12669 (2002)] and for the cw bias [P. Cluzel *et al.*, Science **287**, 1652 (2000)], which plausibly may be identified as the fraction of protomers realizing state 2. Finally, the relationships between our analytical results and the classical Monod-Wyman-Changeaux, Koshland-Nemethy-Filmer, and McGhee-Von Hippel treatments of allosteric cooperativity are elucidated, as is the connection to an earlier approximate analytical treatment of the CS model.

DOI: 10.1103/PhysRevE.82.031913 PACS number(s): 87.15.A−, 87.50.cf, 82.35.Pq

I. INTRODUCTION

Allosteric cooperativity is widespread in biology as a means of creating a molecular switch [1–4]. The classical Monod-Wyman-Changeaux (MWC) treatment [1] was developed to account for the sigmoidal oxygen-binding behavior of tetrameric hemoglobin as a function of blood oxygen concentration. More recently, Duke and co-workers [5,6] introduced a more general, and physically appealing, model for allosteric transitions in a ring of N identical so-called "protomers," driven by ligand binding. Introduction of this model was motivated in part by a desire to better understand the bacterial flagellar motor, for which the protomers correspond to FliM/FliG/FliN protein complexes, which form a 34-membered ring [7], whose conformation is believed to determine whether the bacterial flagellar motor turns clockwise or counterclockwise. In turn, this conformation is coupled to ligand binding, where the ligands in question are the chemotaxis signaling proteins, CheY-P [8–13]. A similar model for the binding of myosin subfragment 1 to the actin-troponin-tropomyosin complex was proposed and analyzed in Ref. [14].

As recognized by Duke *et al.*, their model is also applicable to linear systems. In particular, it may be applicable in the case of DNA-binding ligands, for which cooperativity of binding is the result of an induced allosteric change in the DNA structure [15]. Possible realizations of such a scenario include DNA binding by netropsin and distamycin [15], histone protein H1 [16–18], and Rad51 [19]. It may also be applicable to the binding of proteins in the actin depolymering factor (ADF/cofilin) family to actin filaments (F-actin) [20–30].

In their model, Duke *et al.* envision a ring or line of N protomers—each of which possesses a ligand binding site—in diffusive equilibrium with a solution containing a concentration c of ligands. Each protomer can exist in one of two allosteric states, which we call states 1 and 2. Each of these two allosteric states can either bind a ligand or not bind a ligand. Thus, each protomer can be conceived as being in one of four possible states: state 1 without ligand bound, state 2 without ligand bound, state 1 with ligand bound, and state 2 with ligand bound. In the absence of ligand, state 1 has a lower free energy than state 2. However, this situation is reversed upon ligand binding: state 2 with ligand bound has a lower free energy than state 1 with ligand bound. Thus, state 2 has a higher ligand binding affinity than state 1. In addition, for protomers arranged around a ring or along a line, Duke *et al.* envision a free-energy cost for nearest-neighbor protomers that realize different allosteric states, i.e., the free energy of a configuration in which a protomer in state 1 neighbors a protomer in state 2 is greater than the free energy of a configuration in which neighboring protomers are both in state 1 or both in state 2. This contribution to the free energy introduces cooperativity into the model and tends to lead to runs around the ring, or along the line, of the same allosteric state. Following Duke *et al.*, henceforth, we refer to this model as the conformational spread (CS) model. In Ref. [5], Duke *et al.* determined the statistical-mechanical behavior of the one-dimensional version of the CS model in a ring geometry via Monte Carlo simulation for a ring of 34 protomers and via an approximate analytical treatment. The two-dimensional version of the CS model, discussed in Ref. [6], is beyond the scope of this paper.

Here, we present an analysis of the CS model via a one-dimensional transfer matrix approach [31] for calculating the statistical-mechanical grand partition function [32]. Our treatment permits us straightforwardly to derive expressions for a number of key quantities of interest, including in particular the fraction of ligand-bound protomers and the frac-

tion of protomers in each allosteric state as a function of ligand concentration, for an arbitrary number (N) of protomers in a ring or along a line. Our motivation is to provide analytical results, which are exact within the context of the model, and which we expect will prove valuable for describing experimental data in a variety of situations. In particular, it will no longer be necessary to resort to Monte Carlo simulations to display this model's properties [13]. To demonstrate the utility of our solution in a biological context of considerable interest, we have fit our analytical predictions to experimental results obtained on the bacterial flagellar motor for, on one hand, the fraction of FliM/FliG/FliN complexes with CheY-P bound, taken from Ref. [10], and for, on the other, the cw bias, taken from Ref. [9], which plausibly may be identified as the fraction of protomers realizing state 2. Simultaneous least-mean-square fits to these two sets of data yield consensus best-fit parameters that provide a good description of both sets of data. We also show that the CS model is consistent with ADF/cofilin-actin binding data. Beyond the expressions we give explicitly, our choice of method publicizes an accessible framework that others will be able to adapt to their own needs. We also elucidate the character of the approximate solution of the CS model, presented by Duke *et al.* [5], and how the CS model reduces in one limit to the MWC model [1], and in another limit to the Koshland-Nemethy-Filmer (KNF) model [2]. Matrix methods have previously been employed to address related questions in Refs. [14,15,33–38], for example.

II. STATISTICAL MECHANICS

To derive the appropriate transfer matrix, initially, we consider a single isolated protomer. Statistical mechanics then informs us [32] that the grand partition function is

$$Z = 1 + L + cK_1 + cK_2L, \tag{1}$$

where the zero of the free energy is defined to correspond to the free energy of an isolated protomer in state 1, L is the equilibrium constant for the transition from state 1 to state 2 in the absence of ligand binding, c is the concentration of ligand, K_1 is the ligand binding affinity in state 1, and K_2 is the ligand binding affinity in state 2. This notation is similar to that ordinarily used in discussions of the MWC model, except that we substitute states 1 and 2 for the relaxed and tense states, respectively. Equation (1) may be rewritten as

$$Z = \mathbf{V} \cdot \mathbf{W}, \tag{2}$$

where

$$\mathbf{W} = \begin{pmatrix} 1 \\ L \\ cK_1 \\ cK_2L \end{pmatrix}, \tag{3}$$

$$\mathbf{V} = (1 \quad 1 \quad 1 \quad 1). \tag{4}$$

Next, we consider two neighboring protomers. In this case, the grand partition function may be easily seen to be

$$Z = 1 + 2cK_1 + c^2K_1^2 + 2LJ + 2cK_1LJ + 2cK_2LJ + 2c^2K_1K_2LJ + L^2 + 2cK_2L^2 + c^2K_2^2L^2, \tag{5}$$

where J is the equilibrium constant associated with the "domain wall" between a state 1 protomer and a state 2 protomer. We expect that usually $0<L<1$, $K_2L>K_1>0$, and $0<J\leq 1$, implying that state 2 is less likely to be realized than state 1 in the absence of binding, that state 2 has a sufficiently higher binding affinity than state 1 for ligand binding to state 2 to be able to drive the transition, and that the system is cooperative with like neighbors favored. However, in principle, the following calculations are valid for arbitrary positive values of these parameters. They are also valid for arbitrary values of the number of protomers (N) in the line segment or ring under consideration. We may relate our parameters to those employed in Refs. [5,13], namely, E_A and E_J, via $L=e^{-\beta E_A}$, $J=e^{-\beta E_J}$, and $K_2/K_1=e^{2\beta E_A}$ with $\beta=(k_BT)^{-1}$, and $E_A>0$ and $E_J>0$. The implied relationship between L and K_2/K_1, i.e., that $L^2=K_1/K_2$, was imposed in Refs. [5,13] for convenience. However, as these authors recognized, this condition is by no means required and has no physical basis in general, although they do suggest that the symmetric case is especially advantageous for creating a molecular switch.

We can rewrite Eq. (5) as the matrix equation

$$Z = \mathbf{V} \cdot \mathbf{T} \cdot \mathbf{W}, \tag{6}$$

where

$$\mathbf{T} = \begin{pmatrix} 1 & J & 1 & J \\ LJ & L & LJ & L \\ cK_1 & cK_1J & cK_1 & cK_1J \\ cK_2LJ & cK_2L & cK_2LJ & cK_2L \end{pmatrix} \tag{7}$$

is the transfer matrix. More generally, the transfer matrix relates the grand partition function for a segment of $N-1$ protomers to the grand partition function for a segment of N protomers. Thus, for a segment of N protomers the grand partition function is found by repeated application of the transfer matrix and is explicitly given by

$$Z = \mathbf{V} \cdot \mathbf{T}^{N-1} \cdot \mathbf{W}. \tag{8}$$

Similarly, for a loop of N protomers,

$$Z = \mathrm{Tr}(\mathbf{T}^N), \tag{9}$$

where Tr denotes the matrix trace.

Given the grand partition function, it is straightforward to calculate the corresponding fraction of ligand-binding sites actually occupied by bound ligands (f), using the statistical-mechanical result that

$$f = \frac{c}{N}\frac{\partial \ln Z}{\partial c}. \tag{10}$$

It is likewise straightforward to calculate the fraction of protomers in state 2,

$$f_2 = \frac{L}{N}\frac{\partial \ln Z}{\partial L}, \tag{11}$$

and the mean number of state 1-to-state 2 boundaries per protomer,

$$f_{12} = \frac{J}{N}\frac{\partial \ln Z}{\partial J}. \tag{12}$$

III. RESULTS AND DISCUSSION

The utility of Eqs. (8) and (9) is that the grand partition function may be straightforwardly evaluated by diagonalizing the transfer matrix. Thus, for N protomers arranged in a loop, the grand partition function is especially simple:

$$Z = \mathrm{Tr}(\mathbf{T}^N) = \lambda_1^N + \lambda_2^N + \lambda_3^N + \lambda_4^N, \tag{13}$$

where λ_1, λ_2, λ_3, and λ_4 are the eigenvalue of $\mathbf{T}$. For the transfer matrix given by Eq. (7), we have

$$\lambda_1 = \tfrac{1}{2}\{1 + cK_1 + L + cK_2L + \sqrt{[(-1 - cK_1 - L - cK_2L)^2 - 4(L - J^2L + cK_1L - cJ^2K_1L + cK_2L - cJ^2K_2L + c^2K_1K_2L - c^2J^2K_1K_2L)]}\}, \tag{14}$$

$$\lambda_2 = \tfrac{1}{2}\{1 + cK_1 + L + cK_2L - \sqrt{[(-1 - cK_1 - L - cK_2L)^2 - 4(L - J^2L + cK_1L - cJ^2K_1L + cK_2L - cJ^2K_2L + c^2K_1K_2L - c^2J^2K_1K_2L)]}\}, \tag{15}$$

$$\lambda_3 = 0, \tag{16}$$

$$\lambda_4 = 0. \tag{17}$$

For a ring, containing N protomers, we give explicit expressions for f [Eq. (A1)] and f_2 [Eq. (A2)] in the Appendix. In the limit of infinite N, Eqs. (A1) and (A2) become dominated by the largest eigenvalue, corresponding to an infinite ring or infinite line of protomers. These collected expressions constitute the principal results of this paper. We expect that they will prove useful for describing a variety of experimental measurements [9–11,18,19,26,27] in which cooperative allosteric effects are implicated. Although unwieldy, Eqs. (A1) and (A2) nevertheless may be readily fitted to experimental data, as we show below. The lower panel of Fig. 1 shows the fraction of protomers in state 2 versus ligand concentration, according to Eq. (A2) in the limit of infinite N for three representative sets of parameters, while the upper panel of Fig. 1 illustrates the corresponding fraction of protomers binding ligand versus ligand concentration, according to Eq. (A1). For each set of parameters, the fraction of protomers in state 2 varies in a sigmoidal fashion as a function of ligand concentration: for concentrations less than about $c_0=(K_2L-K_1)/(1-L)$, the fraction of protomers in state 2 (f_2) is very small. It then increases rapidly, soon reaching unity for concentrations greater than c_0. By contrast, the fraction of protomers binding ligand (f) initially varies approximately linearly at small ligand concentrations. It then also increases rapidly near c_0, to a larger value and eventually saturates at a value of unity at large ligand concentrations. Similar contrasting behavior for these two quantities was found in Ref. [5]. In fact, as noted previously [5,13], the behavior of the fraction of protomers binding ligand (f) can be understood at small and large ligand concentrations: at small ligand concentrations, f corresponds to the noncooperative binding by protomers in state 1, i.e., $f \simeq cK_1/(1+cK_1)$. At large ligand concentrations, nearly all of the protomers realize state 2, and f corresponds to the noncooperative binding by protomers in state 2, i.e., $f \simeq cK_2/(1+cK_2)$. The dashed curves in the upper panel of Fig. 1 correspond to noncooperative binding by protomers in state 1 (brown), and noncooperative binding by protomers in state 2 (magenta) for theupper, solid brown binding curve. Clearly, the brown curve itself switches between the expected limiting behaviors.

The difference in behavior between, on one hand, the fraction of protomers realizing state 2 and, on the other hand, the fraction of protomers binding ligand is highlighted in Fig. 2, which shows a comparison between the calculated fraction of protomers realizing state 2 (red solid line) and the calculated fraction of protomers binding ligand (blue solid line) versus ligand concentration. The parameters used to make these plots are $L=e^{-1.32}=0.517$, $J=e^{-4.13}=0.016$, $K_1=e^{-0.66}/(3.1\ \mu\mathrm{M})=0.167\ \mu\mathrm{M}$, $K_2=e^{0.66}/(3.1\ \mu\mathrm{M})=0.624\ \mu\mathrm{M}$, and $N=34$, corresponding to $\beta E_A=0.66$ and $\beta E_J=4.13$, which are the values used in the Monte Carlo simulations of Ref. [13]. Comparison between our exact calculations (Fig. 2) and the results of Monte Carlo simulations, shown in Fig. 4(D) of Ref. [13], reveals excellent agreement between these two approaches.

Also shown in Fig. 2 are two sets of experimental data. The first set of data (blue squares) is taken from Fig. 2(B) of Ref. [10] and corresponds to the fraction of FliM/FliG/FliN complexes with CheY-P bound (blue squares), i.e., the fraction of protomers binding ligand. Similar results have been presented in Ref. [11]. The second set of data (red circles) is taken from Fig. 2(A) of Ref. [9] and corresponds to the cw bias (red circles), which plausibly may be identified as the fraction of protomers realizing state 2. Although these data are noisy, they appear to be qualitatively described by our calculations, based on the parameters given in Ref. [13]. In addition, however, even better agreement may be achieved

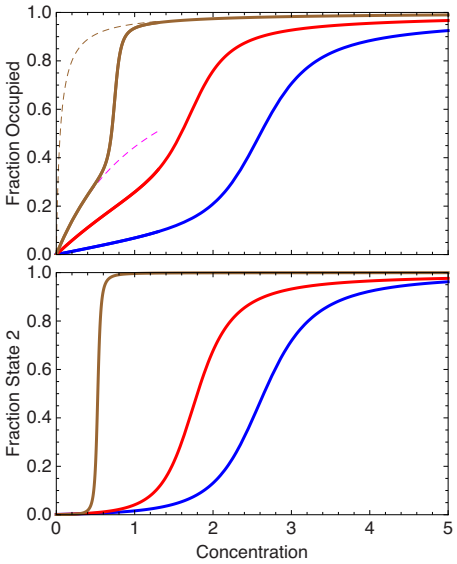

FIG. 1. (Color online) Top: fraction of protomers with ligand bound in the large-N limit vs ligand concentration for three sets of parameters, namely, $L=0.1$, $J=0.03$, $K_1=0.8$, and $K_2=20$ for the brown (upper) curve; $L=0.1$, $J=0.08$, $K_1=0.3$, and $K_2=8$ for the red (middle) curve; and $L=0.1$, $J=0.1$, $K_1=0.06$, and $K_2=4$ for the blue (lowest) curve. The fact that the fraction of protomers with ligand bound may be understood as a crossover from noncooperative binding by protomers in state 1 at low concentration to noncooperative binding by protomers in state 2 at high concentration is illustrated in the case of the brown curve by the dashed curves, which show the expected limiting behaviors at low and high concentrations. Bottom: fraction of protomers realizing state 2 in the large-N limit vs ligand concentration for the same three sets of parameters as in the top panel.

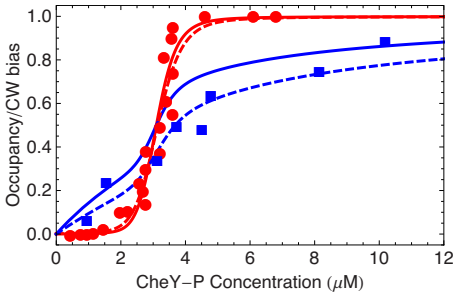

FIG. 2. (Color online) Comparison between the fraction of protomers realizing state 2 (red [upper-at-right] solid line) and the fraction of protomers binding ligand (blue [lower-at-right] solid line) versus ligand concentration for $L=e^{-1.32}=0.517$, $J=e^{-4.13}=0.016$, $K_1=e^{-0.66}/(3.1\ \mu\text{M})=0.167\ \mu\text{M}$, $K_2=e^{0.66}/(3.1\ \mu\text{M})=0.624\ \mu\text{M}$, and $N=34$. These parameters correspond to $\beta E_A=0.66$ and $\beta E_J=4.13$, which were the values deduced in Ref. [13]. Also plotted are the results for the cw bias of the bacterial flagellar motor, taken from Ref. [9] (red circles), and for the fractional CheY-P occupancy of FliM, taken from Ref. [10] (blue squares). Choosing $1/\sqrt{K_1K_2}=3.1\ \mu\text{M}$ ensures a match between the theory and experimental [9] ligand concentrations at which one half of the protomers are in state 1 and one half are in state 2. The dashed lines show the results of a simultaneous least-mean-square fit of our model to these two data sets. The corresponding best-fit parameters are $L=0.636\pm0.116$, $J=0.0188\pm0.032$, $K_1=0.104\pm0.053\ \mu\text{M}$, and $K_2=0.345\pm0.070\ \mu\text{M}$.

by carrying out a simultaneous least-mean-square fit of our model [Eqs. (A1) and (A2) for $N=34$] to these two data sets, as shown by the dashed lines, which correspond to the best-fit model curves. Thus, the CS model is able to provide a good description of these two different experimental quantities with a single set of consensus fitting parameters, namely, $L=0.636\pm0.116$, $J=0.0188\pm0.032$, $K_1=0.104\pm0.053\ \mu\text{M}$, and $K_2=0.345\pm0.070\ \mu\text{M}$. These parameters deviate slightly from the assumption of Refs. [5,13] that $L^2=K_1/K_2$. Here, we find that $L^2=0.404$ while $K_1/K_2=0.301$.

The CS model may also be relevant in the context of actin binding by proteins in the actin depolymerizing factor/cofilin (ADF/cofilin) family [20–29]. The starting points for our discussion of ADF/cofilin-actin binding is, first, the observation that literature examples of ADF/cofilin-to-actin binding curves are highly variable, depending on the particular actin and ADF/cofilin employed in each case. For example, Refs. [23,25] report noncooperative binding, while in Refs. [22,26], for example, actin-cofilin binding is well described by a highly cooperative model. Second, electron microscopy (EM) measurements reveal that neighboring ADF/cofilins bound to F-actin are not in physical contact and that actin with bound ADF/cofilin shows a helical pitch about 75% that of naked actin [22]. These observations immediately lead to the proposal that cooperativity in the binding of ADF/cofilin to actin may be expected to originate via this structural change in the actin filament and does not originate from direct interactions between ADF/cofilins, just as hypothesized in the CS model. In addition, in a more recent EM study, Bobkov *et al.* reported that "segments of pure actin can be found in an ADF/cofilin-like state of twist in the absence of other proteins," i.e., a state with a 45 nm helical pitch (state 2), and that "the ADF-actin complex can exist with a twist close to that of the normal actin state," i.e., a state with a 72 nm helical pitch (state 1). The conclusions from EM indeed seem consistent with a CS model for ADF/cofilin-actin binding. According to this point of view, the ADF/cofilin-actin system displays four states: actin in state 1 with no cofilin bound, actin in state 1 with cofilin bound,

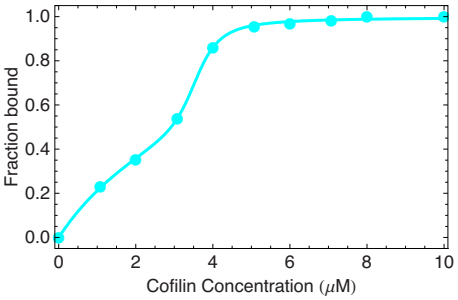

FIG. 3. (Color online) Actin-cofilin binding described by the CS model. The circles, taken from Ref. [28], illustrate the fraction of actin sites that bind cofilin, as a function of cofilin concentration. The best-fit parameters are $K_1=0.265\pm0.009$, $K_2=23.11\pm17.71$, $L=0.023\pm0.018$, and $J=0.047\pm0.005$.

actin in state 2 with cofilin bound, and actin in state 2 with no cofilin bound. The fact that the measured binding curves are variable from realization to realization suggests a corresponding variability in binding affinities for different realizations of ADF/cofilin-actin. In particular, we hypothesize that for cases in which the binding appears to be noncooperative, K_1 is not too much smaller than K_2, reminiscent of CheY-P binding (blue curves in Fig. 2), while for cases in which the binding appears cooperative, K_1 is much smaller than K_2. We compare the CS model's prediction to one example of an experimental binding curve in Fig. 3. The circles in this figure, taken from Ref. [28], illustrate the fraction of actin sites that bind cofilin, as a function of cofilin concentration. The solid line shows the corresponding best fit of the CS model predictions in the infinite-N limit to this data set. Evidently, the fit provides an excellent description of these measurements. The corresponding best-fit parameters are $K_1 = 0.265 \pm 0.009$, $K_2 = 23.11 \pm 17.71$, $L = 0.023 \pm 0.018$, and $J = 0.047 \pm 0.005$.

Equations (A1) and (A2) are both exact within the context of the CS model. However, we may make contact with a number of additional results in the literature by considering the CS model in certain limits. In particular, as may be expected, the $J=0$ limit of Eq. (13), corresponding to infinite cooperativity, leads to the well-known MWC model result for the grand partition function, namely,

$$Z = (1 + cK_1)^N + L^N(1 + cK_2)^N. \tag{18}$$

An improvement upon the MWC expression [Eq. (18)] may be achieved by including in the grand partition function configurations with n tandem protomers in state 1 and $N-n$ tandem protomers in state 2. This approximation is analogous to the zipper treatment of the one-dimensional Ising model [39] and represents the first term in a series expansion of the grand partition function in powers of J^2. It follows that the MWC expression requires J^2N to be sufficiently small in order for it to be a good approximation. Specializing to a ring of N protomers, the zipper approximation for the grand partition function of the CS model is readily written down as

$$Z = (1 + cK_1)^N + L^N(1 + cK_2)^N + NJ^2 \sum_{n=1}^{n=N-1} (1 + cK_1)^n (1 + cK_2)^{N-n} L^{N-n} = (1 + cK_1)^N + (1 + cK_2)^N L^N$$
$$- \frac{J^2[-(1 + cK_1)^N L - c(1 + cK_1)^N K_2 L + (1 + cK_2)^N L^N + cK_1(1 + cK_2)^N L^N]N}{1 + cK_1 - L - cK_2 L}. \tag{19}$$

Zipper-approximation expressions for f and f_2 follow from the application of Eqs. (10) and (11), respectively. Here, we content ourselves with supplying the result for f_2, namely,

$$f_2 = \left(L \left\{ (1 + cK_2)^N L^{-1+N} + \frac{J^2(1 + cK_2)[(1 + cK_1)^N(1 + cK_2)L - (1 + cK_1)(1 + cK_2)^N L^N]}{(-1 - cK_1 + L + cK_2 L)^2} \right.\right.$$
$$\left.\left. + \frac{J^2[-(1 + cK_1)^N(1 + cK_2)L + (1 + cK_1)(1 + cK_2)^N L^N N]}{L(-1 - cK_1 + L + cK_2 L)} \right\} \right) \Bigg/ \left\{ (1 + cK_1)^N + (1 + cK_2)^N L^N \right.$$
$$\left. - \frac{J^2[-(1 + cK_1)^N(1 + cK_2)L + (1 + cK_1)(1 + cK_2)^N L^N]N}{1 - L + c(K_1 - K_2 L)} \right\}. \tag{20}$$

Equation (20) is equivalent to the result given as Eq. (A9) in Ref. [5], provided we identify λ of Ref. [5] via $\lambda = (1 + cK_2)L/(1 + cK_1)$. The zipper-approximation results (Eqs. (20) and (A9) of Ref. [5], etc.) are themselves expected to be valid only for $J^2N \ll 1$. The fact that there can be noticeable discrepancies between the exact results and the zipper approximation, even for $J^2N \simeq 0.05$, is illustrated in Fig. 4, which shows, for a 34-membered ring of protomers with $J = 0.04$, the fraction of protomers realizing state 2 as a function of ligand concentration. The red curve shows the exact transfer matrix result. The blue curve shows the zipper-approximation result. Evidently, the zipper-approximation result shows a sharper variation versus ligand concentration than the exact result.

Alternatively, consideration of Eqs. (7) and (A1) in the limit that $K_1 \to 0$, $L \to 0$, and $K_2 \to \infty$, while $K = K_2 L$ remains finite and nonzero, informs us that in this case, the allosteric state of the protomer is completely tied to whether or not a ligand is bound, i.e., either the protomer is in state 1 with no ligand bound or the protomer is in state 2 with ligand bound. This situation corresponds to the KNF picture of allostery [2]. The transfer matrix in this case reduces to a 2×2 form,

$$\mathbf{T} = \begin{pmatrix} 1 & J \\ JcK & cK \end{pmatrix}, \tag{21}$$

corresponding to the two possible protomer states. Following the same steps as above, we may readily determine the corresponding fraction of binding sites occupied, also known as the fraction of protomers in state 2,

$$f = f_2 = \frac{c\left(K + \frac{K(-1+cK+2J^2)}{\sqrt{1+c^2K^2+2cK(-1+2J^2)}}\right)}{1+cK+\sqrt{1+c^2K^2+2cK(-1+2J^2)}}. \quad (22)$$

Not surprisingly, given that it is a two-state model with two parameters, the model described by Eqs. (21) and (22) is equivalent to the classic one-dimensional nearest-neighbor Ising model or, equivalently, the Zimm-Bragg model [31,40–43]. It is also equivalent to the McGhee-Von Hippel model [26,44,45] in the case that there is one ligand binding site per protomer ($n=1$ in Eq. (15) of Ref. [44]): solving Eq. (15) of Ref. [44] for the fraction of protomers bound to ligand leads to the expression

$$f = \frac{1+4c\kappa-2c\kappa\omega+c^2\kappa^2\omega^2+(-1+c\kappa\omega)\sqrt{1+4c\kappa-2c\kappa\omega+c^2\kappa^2\omega^2}}{2(1+4c\kappa-2c\kappa\omega+c^2\kappa^2\omega^2)}, \quad (23)$$

which, in turn, is exactly equivalent to Eq. (22), provided we identify $\omega=J^{-2}$ and $\kappa=KJ^2$.

In the KNF limit just considered, it is immaterial whether or not the cooperativity parameter (J) derives from interactions between protomers or ligands. In the original CS model, there is no provision for direct interactions between ligands. However, it is straightforward to incorporate into the transfer matrix an additional free-energy cost, with corresponding equilibrium constant w associated with configurations containing neighboring protomers, one with a ligand bound and the other without ligand bound:

$$\mathbf{T} = \begin{pmatrix} 1 & J & w & Jw \\ LJ & L & LJw & Lw \\ cK_1w & cK_1Jw & cK_1 & cK_1J \\ cK_2LJw & cK_2Lw & cK_2LJ & cK_2L \end{pmatrix}. \quad (24)$$

The four eigenvalues of the matrix in Eq. (24) are the roots of quartic equations, and we do not pursue the full consequences of Eq. (24) further.

Within the context of the transfer matrix approach, it is straightforward to calculate the probability that a particular site—site n, say—is in state 2 [31]:

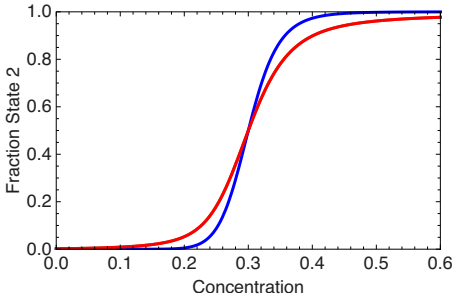

FIG. 4. (Color online) Fraction of protomers realizing state 2 vs ligand concentration, calculated either via the exact transfer matrix method (red [upper-at-left] curve) or via the zipper approximation (blue [lower-at-left] curve). In both cases, the parameters are $L=0.4$, $J=0.04$, $K_1=2.0$, $K_2=10$, and $N=34$.

$$\mathrm{Tr}(\mathbf{T}^{N-n}\cdot\mathbf{P}\cdot\mathbf{T}^{n})/Z, \quad (25)$$

or

$$\mathbf{V}\cdot\mathbf{T}^{N-n}\cdot\mathbf{P}\cdot\mathbf{T}^{n-1}\cdot\mathbf{W}/Z, \quad (26)$$

for a ring or line, respectively, where

$$\mathbf{P} = \begin{pmatrix} 0 & 0 & 0 & 0 \\ 0 & 1 & 0 & 0 \\ 0 & 0 & 0 & 0 \\ 0 & 0 & 0 & 1 \end{pmatrix} \quad (27)$$

is a projection operator. More interestingly, we can calculate the probability that sites n and m are both in state 2:

$$\mathrm{Tr}(\mathbf{T}^{N-m}\cdot\mathbf{P}\cdot\mathbf{T}^{m-n}\cdot\mathbf{P}\cdot\mathbf{T}^{n})/Z, \quad (28)$$

or

$$\mathbf{V}\cdot\mathbf{T}^{N-m}\cdot\mathbf{P}\cdot\mathbf{T}^{m-n}\cdot\mathbf{P}\cdot\mathbf{T}^{n-1}\cdot\mathbf{W}/Z, \quad (29)$$

for a ring or line, respectively. The conditional probability that site m realizes state 2, given that site n realizes state 2, is via Bayes' theorem, the ratio of Eq. (25) to Eq. (28):

$$g = \frac{\mathrm{Tr}(\mathbf{T}^{N-m}\cdot\mathbf{P}\cdot\mathbf{T}^{m-n}\cdot\mathbf{P}\cdot\mathbf{T}^{n})}{\mathrm{Tr}(\mathbf{T}^{N-n}\cdot\mathbf{P}\cdot\mathbf{T}^{n})}, \quad (30)$$

for a ring, or the ratio of Eq. (26) to Eq. (29):

$$g = \frac{\mathbf{V}\cdot\mathbf{T}^{N-m}\cdot\mathbf{P}\cdot\mathbf{T}^{m-n}\cdot\mathbf{P}\cdot\mathbf{T}^{n-1}\cdot\mathbf{W}}{\mathbf{V}\cdot\mathbf{T}^{N-n}\cdot\mathbf{P}\cdot\mathbf{T}^{n-1}\cdot\mathbf{W}}, \quad (31)$$

for a line. How Eq. (30), or Eq. (31), varies as a function of m, n, and N describes how allostery propagates around the ring or along the line in the CS model. Focusing on Eq. (30) for convenience, we have that

$$g = \frac{\mathrm{Tr}(\mathbf{T}^{N-m+n}\cdot\mathbf{P}\cdot\mathbf{T}^{m-n}\cdot\mathbf{P})}{\mathrm{Tr}(\mathbf{T}^{N}\cdot\mathbf{P})}, \quad (32)$$

because the trace is invariant under cyclic permutation. Introducing $\mathbf{Q}$, the projection matrix expressed in the coordinate system in which $\mathbf{T}$ is diagonal, Eq. (32) can be rewritten as

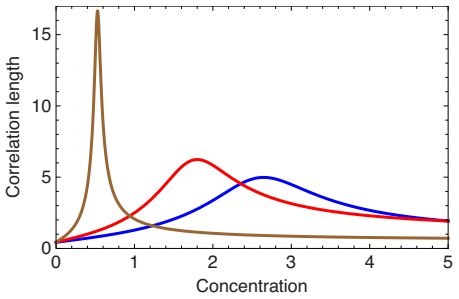

FIG. 5. (Color online) Correlation length versus ligand concentration for the same three sets of parameters as in Fig. 1: $L=0.1$, $J=0.01$, $K_1=0.3$, and $K_2=20$ (brown curve, peak at left); $L=0.1$, $J=0.03$, $K_1=0.2$, and $K_2=12$ (blue curve, peak at right); and $L=0.1$, $J=0.08$, $K_1=0.1$, and $K_2=8$ (red curve, peak in the middle).

$$g = \frac{\mathbf{Q}_{11} + \frac{\mathbf{Q}_{12}\mathbf{Q}_{21}}{\mathbf{Q}_{11}}\left[\left(\frac{\lambda_2}{\lambda_1}\right)^{N-m+n} + \left(\frac{\lambda_2}{\lambda_1}\right)^{m-n}\right] + \frac{\mathbf{Q}_{22}^2}{\mathbf{Q}_{11}}\left(\frac{\lambda_2}{\lambda_1}\right)^N}{1 + \frac{\mathbf{Q}_{22}}{\mathbf{Q}_{11}}\left(\frac{\lambda_2}{\lambda_1}\right)^N}, \tag{33}$$

where $\mathbf{Q}_{ij}$ is the ij element of $\mathbf{Q}$. The first and the last terms on the right-hand side are evidently independent of separation. Together they yield the probability that protomer m is in state 2 irrespective of whether protomer n realizes state 2 or not. By contrast, the second term indeed depends on $(n-m)$. For $m-n \ll N$, the second term decreases exponentially with $m-n$ over a characteristic distance scale, or correlation length, given by $\xi = 1/\ln(\lambda_1/\lambda_2)$, as expected [46]. The correlation length may be interpreted as the range over which setting the conformational state at one location can be expected to affect the conformational state at a distant location (Fig. 5). Thus, for a ring of protomers, if the concentration is such that ξ is greater than N, we may expect switching of a single protomer from state 1 to state 2 usually to cause the entire ring to also switch from state 1 to state 2, and vice versa.

IV. CONCLUSIONS

We have described a transfer matrix method for analyzing the statistical properties of the CS model of allosteric cooperativity within a one-dimensional arrangement—a ring or a line—of four-state protomers. Each protomer can realize one of two possible conformational states, each of which can either bind ligand or not bind ligand. Thus, we derived analytical expressions that are exact within the context of the CS model, for the grand partition function, for the mean fraction of protomers occupied by ligand versus ligand concentration, and for the mean fraction of protomers in a given allosteric state versus ligand concentration. The analytical results derived were related both to the classical Monod-Wyman-Changeaux [1], Koshland-Nemethy-Filmer [2], and McGhee-Von Hippel [44,45] treatments of allosteric cooperativity and to the approximate analytical treatments of the CS model given by Duke *et al.* [5]. We also fit our analytical predictions to experimental results obtained on the bacterial flagellar motor for the fraction of FliM/FliG/FliN complexes with CheY-P bound, taken from Ref. [10], and for the cw bias, taken from Ref. [9], which may be identified as the fraction of protomers realizing state 2. Simultaneous least-mean-square fits to these two sets of data yield consensus best-fit parameters that provide a good description of both sets of data. We also showed that the CS model is consistent with one example of experimental ADF/cofilin-actin binding data.

ACKNOWLEDGMENTS

S.G.J.M and L.R. gratefully acknowledge the Raymond and Beverly Sackler Institute for Biological, Physical and Engineering Science for support. S.G.J.M. thanks Thierry Emonet for introducing him the bacterial flagellar motor, Enrique De La Cruz and Tom Pollard for very valuable comments and discussions, and the participants of the Yale Soft Matter Journal Club, and especially Holger Kress, for rekindling his interest in the CS model.

APPENDIX: EXPLICIT RESULTS

Explicit expressions for f and f_2 for a ring of N protomers are

$$\begin{aligned}
f = [&c((K_1 + K_2L + \{-cK_1^2 - K_2L(-1 + 2J^2 + L + cK_2L) - K_1[1 + (-1 + 2J^2)(1 \\
&+ 2cK_2)L]\}/\{\sqrt{4(-1 + J^2)(1 + cK_1)(1 + cK_2)L + [1 + L + c(K_1 + K_2L)]^2}\})\{1 + cK1 + L + cK2L \\
&- \sqrt{4(-1 + J^2)(1 + cK_1)(1 + cK_2)L + [1 + L + c(K_1 + K_2L)]^2}\}^{N-1} + (K_1 + K_2L + \{cK_1^2 + K_2L(-1 + 2J^2 + L + cK_2L) \\
&+ K_1[1 + (-1 + 2J^2)(1 + 2cK_2)L]\}/\{\sqrt{4(-1 + J^2)(1 + cK_1)(1 + cK_2)L + [1 + L + c(K_1 + K_2L)]^2}\})\{1 + cK_1 + L + cK_2L \\
&+ \sqrt{4(-1 + J^2)(1 + cK_1)(1 + cK_2)L + [1 + L + c(K_1 + K_2L)]^2}\}^{N-1})]/[(1 + L + c(K_1 + K_2L) \\
&- \sqrt{\{1 - 2L + 4J^2L + L^2 + c^2[K_1^2 + 2(-1 + 2J^2)K_1K_2L + K_2^2L^2] + 2c[K_2L(-1 + 2J^2 + L) + K_1(1 - L + 2J^2L)]\}})^N \\
&+ (1 + L + c(K_1 + K_2L) \\
&+ \sqrt{\{1 - 2L + 4J^2L + L^2 + c^2[K_1^2 + 2(-1 + 2J^2)K_1K_2L + K_2^2L^2] + 2c[K_2L(-1 + 2J^2 + L) + K_1(1 - L + 2J^2L)]\}})^N],
\end{aligned} \tag{A1}$$

$$f_2 = \Bigg[L\Bigg(\Bigg\{1 + cK_2 - \frac{(1+cK_2)[-1-cK_1+2J^2(1+cK_1)+L+cK_2L]}{\sqrt{4(-1+J^2)(1+cK_1)(1+cK_2)L+[1+L+c(K_1+K_2L)]^2}}\Bigg\}\{1+cK_1+L+cK_2L$$
$$-\sqrt{4(-1+J^2)(1+cK_1)(1+cK_2)L+[1+L+c(K_1+K_2L)]^2}\}^{N-1} + ((1+cK_2)\{1+cK_1+L+cK_2L$$
$$+\sqrt{4(-1+J^2)(1+cK_1)(1+cK_2)L+[1+L+c(K_1+K_2L)]^2}\}^{N-1}\{-1+2J^2-cK_1+2cJ^2K_1+L+cK_2L$$
$$+\sqrt{4(-1+J^2)(1+cK_1)(1+cK_2)L+[1+L+c(K_1+K_2L)]^2}\})/$$
$$\{\sqrt{4(-1+J^2)(1+cK_1)(1+cK_2)L+[1+L+c(K_1+K_2L)]^2}\}\Bigg)\Bigg] \Big/ [(1+L+c(K_1+K_2L)$$
$$-\sqrt{\{1-2L+4J^2L+L^2+c^2[K_1^2+2(-1+2J^2)K_1K_2L+K_2^2L^2]+2c[K_2L(-1+2J^2+L)+K_1(1-L+2J^2L)]\}})^N$$
$$+(1+L+c(K_1+K_2L)$$
$$+\sqrt{\{1-2L+4J^2L+L^2+c^2[K_1^2+2(-1+2J^2)K_1K_2L+K_2^2L^2]+2c[K_2L(-1+2J^2+L)+K_1(1-L+2J^2L)]\}})^N], \quad \text{(A2)}$$

respectively.

[1] J. Monod, J. Wyman, and J.-P. Changeux, J. Mol. Biol. **12**, 88 (1965).
[2] D. E. Koshland, G. Nemethy, and D. Filmer, Biochemistry **5**, 365 (1966).
[3] J. Wyman and S. J. Gill, *Binding and Linkage: Functional Chemistry of Biological Macromolecules* (University Science Books, Mill Valley, CA, 1990).
[4] D. S. Goodsell and A. J. Olsen, Annu. Rev. Biophys. Biomol. Struct. **29**, 105 (2000).
[5] T. A. Duke, N. A. L. Novere, and D. Bray, J. Mol. Biol. **308**, 541 (2001).
[6] D. Bray and T. A. Duke, Annu. Rev. Biophys. Biomol. Struct. **33**, 53 (2004).
[7] M. D. Manson, J. Bacteriol. **189**, 291 (2007).
[8] M. Welch, K. Oosawa, S. Aizawa, and M. Eisenbach, Proc. Natl. Acad. Sci. U.S.A. **90**, 8787 (1993).
[9] P. Cluzel, M. Surette, and S. Leibler, Science **287**, 1652 (2000).
[10] V. Sourjik and H. C. Berg, Proc. Natl. Acad. Sci. U.S.A. **99**, 12669 (2002).
[11] Y. Sagi, S. Khan, and M. Eisenbach, J. Biol. Chem. **278**, 25867 (2003).
[12] E. A. Korobkova, T. Emonet, H. Park, and P. Cluzel, Phys. Rev. Lett. **96**, 058105 (2006).
[13] F. Bai, R. W. Branch, D. V. Nicolau, T. Pilizota, B. C. Steel, P. K. Maini, and R. M. Berry, Science **327**, 685 (2010).
[14] T. L. Hill, E. Eisenberg, and L. E. Greene, Proc. Natl. Acad. Sci. U.S.A. **77**, 3186 (1980).
[15] N. Dattagupta, M. Hogan, and D. Crothers, Biochemistry **19**, 5998 (1980).
[16] J. O. Thomas, C. Rees, and J. T. Finch, Nucleic Acids Res. **20**, 187 (1992).
[17] P. H. Draves, P. Lowary, and J. Widom, J. Mol. Biol. **225**, 1105 (1992).
[18] N. M. Mamoon, Y. Song, and S. E. Welman, Biopolymers **77**, 9 (2005).
[19] R. B. Robertson, D. N. Moses, Y.-H. Kwon, P. Chan, P. C. H. Klein, P. Sung, and E. C. Greene, Proc. Natl. Acad. Sci. U.S.A. **106**, 12688 (2009).
[20] S. M. Hayden, P. S. Miller, A. Brauweiler, and J. R. Bamburg, Biochemistry **32**, 9994 (1993).
[21] E. H. Egelman and A. Orlova, J. Struct. Biol. **115**, 159 (1995).
[22] A. McGough, B. Pope, W. Chiu, and A. Weeds, J. Cell Biol. **138**, 771 (1997).
[23] L. Blanchoin and T. D. Pollard, J. Biol. Chem. **274**, 15538 (1999).
[24] V. E. Galkin, A. Orlova, N. Lukoyanova, W. Wriggers, and E. H. Egelman, J. Cell Biol. **153**, 75 (2001).
[25] A. A. Bobkov, A. Muhlrad, K. Kokabi, S. Vorobiev, S. C. Almo, and E. Reisler, J. Mol. Chem. **323**, 739 (2002).
[26] E. M. De La Cruz, J. Mol. Biol. **346**, 557 (2005).
[27] E. Andrianantoandro and T. D. Pollard, Mol. Cell **24**, 13 (2006).
[28] A. A. Bobkov, A. Muhlrad, D. A. Pavlov, K. Kokabi, A. Yilmaz, and E. Reisler, J. Mol. Biol. **356**, 325 (2006).
[29] E. M. De La Cruz and D. Sept, Biophys. J. **98**, 1893 (2010).
[30] J. Pfaendtner, E. M. De La Cruz, and G. A. Voth, Proc. Natl. Acad. Sci. U.S.A. **107**, 7299 (2010).
[31] P. Nelson, *Biological Physics: Energy, Information, Life* (W. H. Freeman, New York, 2003).
[32] C. Kittel and H. Kroemer, *Thermal Physics* (W. H. Freeman, New York, 1980).
[33] T. L. Hill, Nature (London) **274**, 825 (1978).
[34] B. Ramanathan and K. S. Schmitz, Biopolymers **17**, 2171 (1978).
[35] T. L. Hill, E. Eisenberg, and L. E. Greene, Proc. Natl. Acad. Sci. U.S.A. **80**, 60 (1983).
[36] T. Tsuchiya and A. Szabo, Biopolymers **21**, 979 (1982).
[37] W. Bujalowski, T. M. Lohman, and C. F. Anderson, Biopolymers **28**, 1637 (1989).
[38] L. S. Tobacman and C. A. Butters, J. Biol. Chem. **275**, 27587 (2000).

[39] C. R. Cantor and P. R. Schimmel, *Biophysical Chemistry Part III: The Behavior of Biological Macromolecules* (W. H. Freeman, New York, 1980).
[40] E. Ising, Z. Phys. **31**, 253 (1925).
[41] B. H. Zimm and J. K. Bragg, J. Chem. Phys. **31**, 526 (1959).
[42] D. Poland and H. A. Scheraga, *Theory of Helix-Coil Transitions in Biopolymers* (Academic Press, New York, 1970).
[43] T. Kajander, A. Lopez-Cortajarena, E. R. G. Main, S. G. J. Mochrie, and L. Regan, J. Am. Chem. Soc. **127**, 10188 (2005).
[44] J. D. McGhee and P. H. von Hippel, J. Mol. Biol. **86**, 469 (1974).
[45] J. D. McGhee and P. H. von Hippel, J. Mol. Biol. **103**, 679(E) (1976).
[46] J. M. Yeomans, *Statistical Mechanics of Phase Transitions* (Oxford University Press, New York, 1992).